Korea Polymer Journal, Vol. 9, No. 1, pp 20-29 (2001)

Interfacial Properties of Electrodeposited Carbon Fiber/Epoxy Composites using Electro-Micromechanical Techniques and Nondestructive Evaluations

Joung-Man Park* and Sang-Il Lee

Department of Polymer Science & Engineering, Research Center for Aircraft Parts Technology
Gyeongsang National University, Chinju 660-701, Korea

Received September 15, 2000

Abstact: Interfacial adhesion and nondestructive behavior of electrodeposited (ED) carbon fiber reinforced composites were evaluated using electro-micromechanical techniques and acoustic emission (AE). The interfacial shear strength (IFSS) of the ED carbon fiber/epoxy composites was higher than that of the untreated fiber. This might be expected because of the possibility of chemical or hydrogen bonding in an electrically adsorbed polymeric interlayer. The logarithmic electrical resistivity of the untreated single-carbon fiber composite increased suddenly to infinity when fiber fracture occurred, whereas that of the ED composite increased relatively gradually to infinity. This behavior may arise from the retarded fracture time due to enhanced IFSS. In single- and ten-carbon fiber composites, the number of AE signals coming from interlayer failure of the ED carbon fiber composite was much larger than that of the untreated composite. As the number of the each first fiber fractures increased in the ten-carbon fiber composite, the electrical resistivity increased stepwise, and the slope of the logarithmic electrical resistance increased.

Introduction

Interfacial adhesion is an important factor in determining the mechanical performance of fiber-reinforced composites. Interfacial shear strength (IFSS) can be improved by surface modifications such as the introduction of chemical functional groups via electrolytic oxidation,[1] ammonia plasma treatment,[2] or coupling agent application.[3] The electrodeposition (ED) method deposits a polymeric film on a conductive surface (such as a carbon fiber) from a dispersion of colloidal ions in water or another suitable liquid. Iroh[4] studied the amount of absorption as a function of ED treatment condition, and compared the mechanical properties between the untreated- and ED graphite fiber/thermoplastic composites using a short-beam shear test and an Izod impact test. Both the flexural and impact strengths of the ED-treated composites were higher than those of the untreated composites.

*e-mail : jmpark@nongae.gsnu.ac.kr

King[5] investigated the micromechanical properties and the failure surface of ED carbon fiber/liquid crystal polymer composites using a short-beam shear test. For a polyphenylene oxide (PPO) treated carbon fiber composite the interlaminar shear strength (ILSS) was higher, and the failure surface rougher, than for the untreated composite. A correlation of ILSS with the modified surface status in the polypyrrole-treated carbon fiber/epoxy composites was also reported.[6] The ILSS of ED-treated composites increased due to enhanced chemical bonding at the interface, and due to increased fiber surface roughness of the polypyrrole films which form the mechanical interlocking. Park[7] evaluated IFSS and microfailure mechanisms in carbon fiber/epoxy composites by ED treatment using monomeric and polymeric coupling agents with the aid of acoustic emission (AE). IFSS in the ED composite exhibited much higher values, and many more AE event signals occurred from interlayer failure compared to the untreated composite.

Many techniques have been applied to investi-

gate interfacial adhesion in composite materials. The most common micromechanical techniques to evaluate IFSS include the single-fiber pullout test,[8,9] the fragmentation test (also known as the single-fiber composite (SFC) test),[10,11] etc. Recently, several researchers have evaluated the characteristics of composites by the measurement of electrical and micromechanical properties. Yuse[12] used an electrical resistance measurement as one of the intelligent nondestructive testing (NDT) methods. The relationship between electrical resistance and fiber breakage/delamination in carbon fiber reinforced plastic (CFRP) laminates was studied using tensile and fatigue tests.

To provide the correlation between interfacial adhesion and electrical properties, Chung *et al.* measured the contact resistivity of carbon or steel fiber/cement matrix composites using the single-fiber electro-pullout test.[13,14] The electro-micromechanical technique has been studied as an economical new NDT method for monitoring curing characteristics, interfacial properties and nondestructive behavior, because the conductive fiber can act both as a sensor and a reinforcing fiber.[15,16] Prasse[17] studied the correlation of electrical resistance change with the AE characteristics of cross-ply carbon fiber reinforced plastics (CFRP) by cyclic loading.

AE is well known as one of the important NDT method. AE can be used to monitor the fracture behavior of composite materials and many AE parameters can be characterized to aid in understanding the sources of microfailure during the progression of the fracture process. When tensile loading is applied to a composite, the AE signal may occur from fiber fracture, matrix cracking, or debonding at the fiber-matrix interface. AE energy released by fiber fracture could be greater than that associated with debonding or matrix cracking.[11] Park[18] and Ma[19] studied the micromechanical properties and microfailure mechanism of single-carbon fiber composites using AE and fragmentation tests.

In the present study, an electro-micromechanical test and AE were used to evaluate interfacial and electrical properties in addition to microfailure modes of conductive carbon fiber composites. After the ED treatment on the carbon fiber surface, the relationship between electrical resistivity and AE events for different surface treatments was investigated for the single- and ten-carbon fibers/epoxy composites.

Experimental

Materials. Two carbon fibers of 8 μm (Taekwang Industrial Co., Korea) and 18 μm (Mitsubishi Chemical Co., Japan) in diameter were used as conductive reinforcing materials. Table I shows the mechanical and electrical properties of the two types of carbon fibers used in the single-fiber tensile test. Electrical properties were measured using a 32 mm distance between two voltage contacts, whereas mechanical properties were measured using a 20 mm gauge length. Testing specimens were prepared with epoxy resin (YD-128, Kukdo Chemical Co., Korea). Epoxy resin is based on diglycidyl ether of bisphenol-A (DGEBA). Polyoxypropylene diamine (Jeffamine D-400 and D-2000, Huntzman Petrochemical Co.) was used as a curing agent. The flexibility of specimens was controlled by adjusting the relative proportion of D-400 *versus* D-2000. Polybutadienemaleic anhydride (PBMA, Polyscience Inc.) was used as

Table I. Intrinsic Electrical and Mechanical Properties for the Two-Carbon Fiber

Carbon Fiber	Electrical Resistance (Ω)	Electrical Resistivity[c] (Ω·cm) $\times 10^{-4}$	Tensile Strength[d] (MPa)	Elastic Modulus (GPa)	Elongation (%)
8 μm[a]	1.19×10^4 (570)	18.6 (0.9)[e]	2878	175	1.8
18 μm[b]	1.57×10^3 (120)	12.5 (1.0)	1753	201	1.1

[a]PAN-based (Taekwang Industrial Co., Korea).

[b]Coal-Tar Pitch-based (Mitsubishi Chemical Co., Japan).

[c]Measured at 32 mm in voltage contacts.

[d]Measured at 20 mm in gauge length.

[e]Parenthesis is standard deviation.

a polymeric coupling agent to improve IFSS by electrodeposition. The molecular weight of PBMA is in the range of 10,000-15,000 g/mol. The chemical structure of PBMA is as follows:

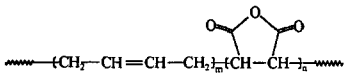

(1)

where m and n are constant.

Methodology

Surface Treatment of Carbon Fiber by ED. Fifty untreated carbon fibers with 8 μm diameter were fixed a suitable distance apart in a rectangular acrylic frame. The carbon fiber acted as an anode, whereas an aluminum plate works as the cathode. PBMA was diluted to 0.5 wt% concentration with deionized water. After the anode and cathode were immersed into aqueous electrolyte solution, 3 volts were supplied to both electrodes by a power supply. The typical coating time was for 10 minutes. After ED treatment, the carbon fibers were dried at room temperature without further thermal treatment.[7]

Preparation of Testing Specimens. As shown in Figure 1, three different types of micro-composite specimens were used for the electro-micromechanical test combined with AE. Figure 1(a) exhibits the testing specimen used to evaluate IFSS as a function of the surface treatment using a two-fiber composite in the absence of electro-micromechanical testing. Figures 1(b) and (c) show the single- and ten-carbon fiber composites used to monitor the electrical resistivity and non-destructive behavior for the combined electro-micromechanical test and AE. In order to avoid the interacting effect between adjacent fibers, the inter-fiber distance was sufficiently separated by a space bar to avoid interactions in the 8 μm carbon fiber composites.[20] A pair of narrow copper wires was fixed transversely on a dogbone-shaped silicone mold, and then single or ten fibers were laid down in a parallel direction unidirectionally. A silver paste electrically connected the intersecting point between the conductive fibers and copper wire. After epoxy resin was poured into the silicone mold, epoxy was precured at 80°C for 2 hours and then postcured at 120°C for 1 hour.

IFSS Measurements. To measure IFSS as a function of the surface treatment and inter-fiber distance, a specially-designed mini-tensile testing machine was used with a polarized-light microscope. After the testing specimen was fixed in the mini-tensile testing machine, the composite was incrementally strained and the fiber was broken into small fragments within the matrix. Load was applied until fiber breaks no longer occurred. The critical fiber fragment length, l_c, was then measured under an optical microscope equipped with a calibrated eyepiece lens.

IFSS was determined using Drzals equation[10,21] that was modified from Kelly-Tyson's equation.[22] By introducing the Weibull distribution for the aspect ratio, IFSS was exhibited in the following form:

$$\tau=\frac{\sigma_f}{2\cdot\alpha}\cdot\Gamma\left[1-\frac{1}{\beta}\right] \quad (2)$$

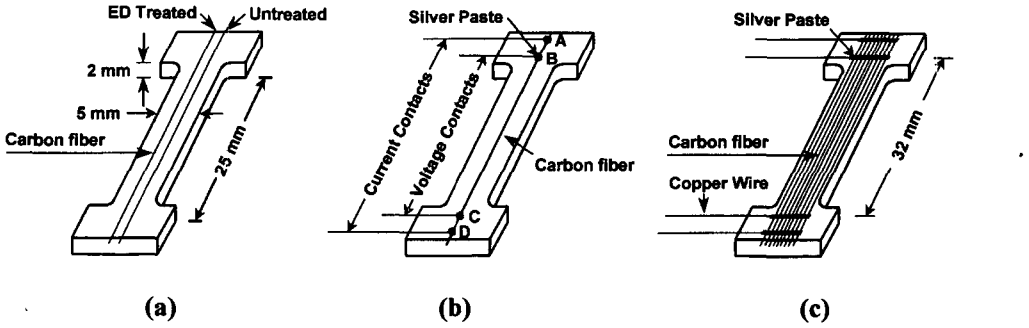

Figure 1. Dimensional scheme of the three types of testing composites for fragmentation, electro-micromechanical test and AE.

Where α and β are scale and shape parameters of the Weibull distribution for aspect ratio (l_c/d), and Γ is the gamma function. Measurement of the fiber tensile strength at the critical fragment length (σ_f, usually less than 1 mm) using a direct tensile test is experimentally difficult due to the short length. Hence, fiber strength was usually determined at the measurable 2 mm gauge length, and was extrapolated to smaller gauge length using the Weibull weakest link rule.[23] The tensile strength at the critical fragment length can be obtained as follows:

$$\sigma_f = \sigma_0 \cdot \left(\frac{l_c}{l_0}\right)^{-\frac{1}{\rho}} \tag{3}$$

where σ_0 is the fiber tensile strength at the measurable gauge length, and ρ is the shape parameter of the Weibull distribution for fiber tensile strength.

Simultaneous Measurements of Mechanical and Electrical Properties. While a tensile load was applied, the electrical resistance was measured using a HP34401A digital multimeter (Figure 2). The stress-strain curve was obtained using a specially-designed tensile testing machine, with a testing speed and load cell of 0.5 mm/minute and 100 kg_f, respectively. After a testing specimen was fixed into the testing grip, the composite and the multimeter were electrically connected using a very thin copper wire. While the tensile load was applied, the electrical resistance and mechanical values of the specimen were simultaneously monitored. Electrical resistivity was obtained from the measured electrical resistance, the cross-sectional area of the conductive fiber

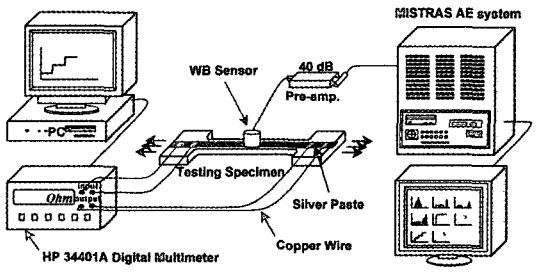

Figure 2. Experimental system for the measurement of electrical resistance and AE signals in carbon fiber composites.

(A), and the electrical contact length (L_{ec}) of the testing fiber connected to copper wire. The relationship between electrical resistivity (ρ) and resistance (R) is as follows:

$$\rho = \left(\frac{A}{L_{ec}}\right) \times R \tag{4}$$

Electrical resistance was measured using a four-point probe method, as shown in Figure 1(b). Silver paste was used as an electrically connecting glue at junctions A, B, C and D to maintain electrical contact between the fiber and leading wire. The voltage was measured between junctions B and C, and the current was measured between junctions A and D. The total electrical resistance (R_{Tot}) between B and C may include R_c, based on the contact resistance of the silver paste, in addition to R_f, due to the electrical resistance of the fiber as follows:

$$R_{Tot} = R_c + R_f \tag{5}$$

Since the value of R_c is negligibly small, due to the very high conductivity of silver paste, compared to R_f, it can be considered that the voltage developed between junctions B and C is very close to the fiber resistance,

$$R_{Tot} \cong R_f \tag{6}$$

AE Measurement. The testing composite was placed on a specially-designed mini-tensile testing machine to apply a unidirectional tensile load. The AE sensor was attached in the center of the testing composite using vacuum grease couplant. AE signals were detected by a miniature sensor (Resonance Type, Model PICO, Physical Acoustics Corporation) with peak sensitivity of 54 Ref. V/(m/s) [-68 Ref. V/mbar] and resonant frequency at 550 kHz. The sensor output was amplified by 40 dB at a preamplifier and passed through a band-pass filter with a range of 200 kHz to 750 kHz. The threshold level was set at 40 dB. The signal was fed into the AE processing unit (MISTRAS 2001 System) and then AE parameters were analyzed (Figure 2). Typical AE parameters such as hit rate, peak amplitude and event energy were investigated in terms of testing time and distribution analysis.

Results and Discussion

IFSS Analysis and AE in Single-Carbon Fiber Composites. In general, the ED process is based on the presence in the polymer of ionizable groups which render it dispersible in water, and which provide the electrical charge for transport when a voltage is applied. Application of an electrical field causes the charged polymer particles to migrate to the electrode surface where they are discharged and coagulate, thus forming a film. By optimizing the treatment parameters, a polymeric coating can be deposited with the desired composition and a homogeneous thickness to improve IFSS.[7]

Table II shows interfacial properties and statistical Weibull parameters for the untreated- and the ED carbon fiber/epoxy composites by the fragmentation test. The average fragment length and aspect ratio of the untreated carbon fiber composite were larger than those of the ED composite. Scale and shape parameters were obtained from the Weibull distribution for aspect ratio of the fiber fragment. The scale parameter of the ED composite was smaller than that of the untreated composite, whereas the shape parameter did not display a significant difference between the cases, which means similar data statistical scattering. In the case of the ED carbon fiber composite, the IFSS exhibited a higher value than for the untreated composite. This may be expected due to chemical and hydrogen bonding between the carbon fiber and epoxy matrix due to the ED treatment.[7,11]

When polymeric PBMA coupling agent is dissolved in distilled water, the ring opening of the maleic anhydride portion can occur through a hydrolysis reaction. The maleic anhydride can be converted into more polar functional groups, such as two carboxyl groups in aqueous solution, as follows:

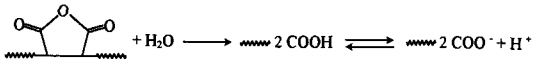

(7)

Figure 3 describes a proposed scheme of possible chemical reactions between carbon fiber and polymeric PBMA coupling agent, as well as between coupling agent and epoxy matrix. There could be hydrogen or chemical bonding at two each interfaces. This bonding might contribute to improving the IFSS and the occurrence of many AE events coming from interfacial microfailure.

Figure 4 shows the adsorption and the desorp-

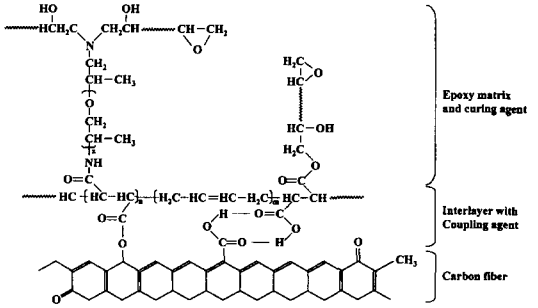

Figure 3. Proposed scheme for possible chemical reactions among carbon fiber, polymeric PBMA coupling agent and epoxy matrix.

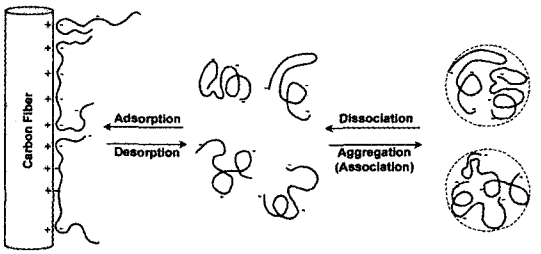

Figure 4. Mechanisms of the adsorption and the desorption between carbon fiber surface and dissolved coupling agent during the ED treatment.

Table II. Comparison of Interfacial Properties and Statistical Weibull Parameters of the Untreated and the ED Carbon Fiber/Epoxy Composites Using a Two-Fiber Fragmentation Test

Surface Treating Condition	Average Fragment Length (μm)	Aspect Ratio (l_c/d)	Scale Parameter (α)	Shape Parameter (β)	IFSS[a] (MPa)
Untreated	620	79 (22)[b]	86.8	3.92	24.9
ED (PBMA)	366	46 (13)	51.2	3.86	52.1

[a]Obtained from Drzals equation.

[b]Parenthesis is standard deviation.

tion mechanism between the carbon fiber surface and the coupling agent dissolved in aqueous solution. It might be possible that there exists an equilibrium between the adsorption and the desorption rates. When a voltage was supplied to the anode and cathode, the carbon fiber might be charged, and the dissolved polymeric coupling agent may become electrolytes such as cations and anions. This coupling agent could give an electron to the carbon fiber in the electrolytic solution and the polymeric coating layer could be adsorbed homogeneously on the fiber surface. This might be considered because electrical attraction might occur and steric hindrance could be induced by chain separation between the coated layers. There will also be some detachment of the attached chains based on steric hindrance of their interaction. On the other hand, coagulation might partially occur in the aqueous solution, and the aggregation and dissociation mechanisms would be the reverse of each other. The adsorption and desorption rates might be relatively low due to the high molecular weight of the polymeric coupling agent.[7]

Figure 5 shows a comparison of the AE amplitude and AE energy as a function of tensile strain for (a) the untreated and (b) the ED carbon fiber composites. The signals for the untreated composite in Figure 5(a) are mainly from fiber fracture, exhibited in terms of AE amplitude and AE energy. On the other hand, many AE signals coming from interlayer failure appeared for the ED case after 16% strain (Figure 5(b)). In addition, the ED carbon fiber exhibited a larger number of fiber fracture signals than that of the untreated composite. Figure 6 shows a comparison of the AE amplitude distribution depending on the testing-time range between the untreated- and ED carbon fiber composites. AE events from the untreated composite did not show any significant difference between initial and later times in Figure 6(a), whereas the ED composite showed a significantly increased low amplitude group of AE events at later time compared with initial time (Figure 6(b)). This behavior might arise from interlayer failure events, and therefore lead to the enhanced IFSS.

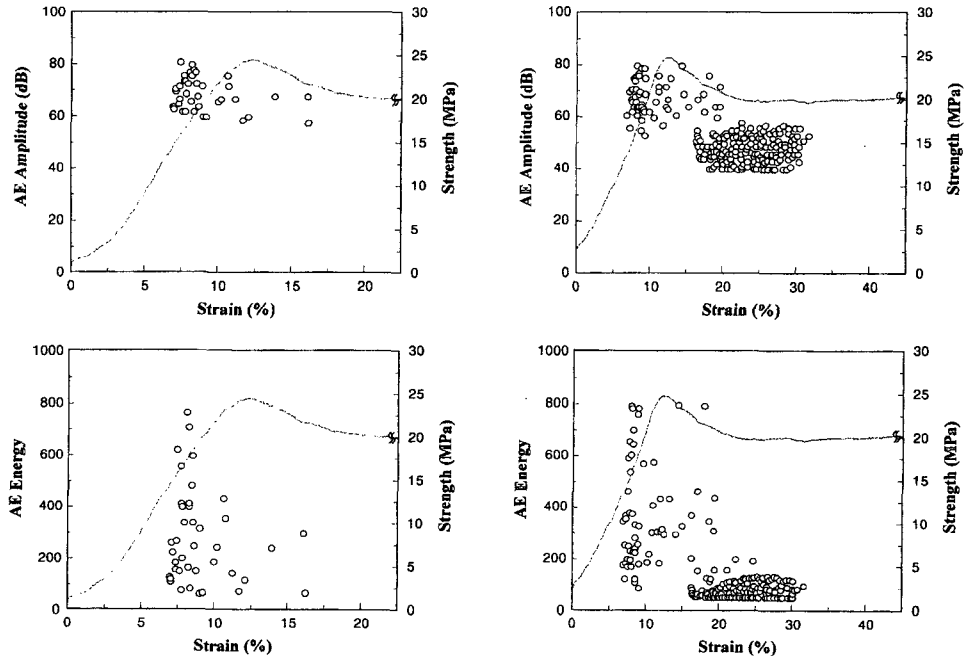

Figure 5. AE amplitude and energy as a function of tensile strain in a single-carbon fiber composite: (a) the untreated; (b) the the ED.

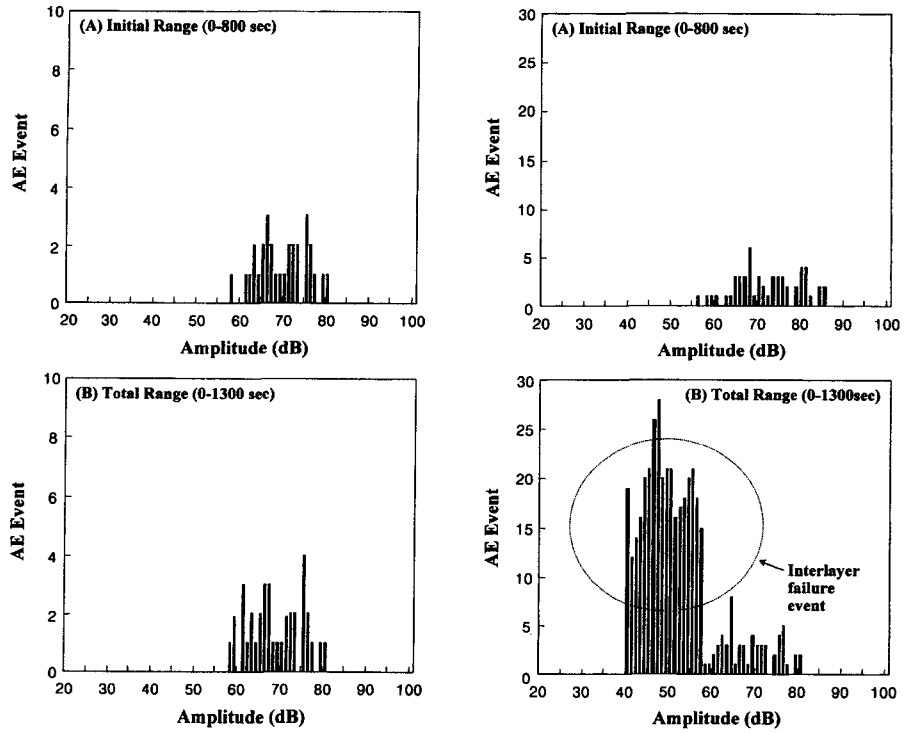

Figure 6. Comparison of amplitude *versus* AE event in a single carbon fiber composite: (a) the untreated; (b) the ED.

Electrical Resistivity of the Untreated and ED Treated Single-Carbon Fiber Composites. Figure 7 shows a comparison between the logarithmic electrical resistivity depending on the ED treatment for single 8 and 18 μm carbon fiber composites. The logarithmic electrical resistivity of the untreated carbon fiber composite increased suddenly compared to the ED carbon fiber composite. This could be because of the retarded fracture time due to improved interfacial adhesion. When tensile stress was transferred from matrix to fiber by an external deformation, a reinforcing fiber could be endured well against the applied tensile stress and could not be easily broken. Precise observation of the shape of the electrical resistivity dependence on fiber diameter shows different trends. When a fiber was broken for the first time, the logarithmic electrical resistivity increased abruptly to infinity in the case of thin 8 μm fiber composite. On the other hand, the electrical resistivity exhibited a smooth increase in the thicker 18 μm carbon fiber composite, until finally the electrical resistivity reached infinity. This behavior might be due mainly to the effect of fiber diameter causing a very abrupt change in

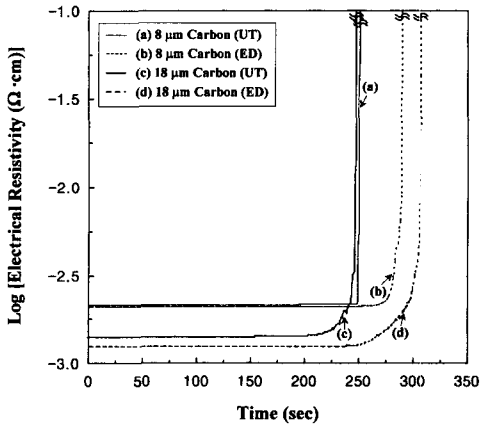

Figure 7. Comparison of logarithmic electrical resistivity depending on the surface treatment and fiber diameter in a SFC: (a) the untreated (8 μm); (b) the ED carbon fiber (8 μm); (c) the untreated (18 μm); and (d) the ED carbon fiber (18 μm).

the electrical resistivity for the thinner 8 μm carbon fiber composite than the thicker 18 μm case.

The trend of the logarithmic electrical resistance for the relatively thin 8 μm carbon fiber composites was different from that of the much thicker 18 μm carbon fibers. This may come from the size effect of fiber diameter in the fiber fracture modes of thin 8 μm and thicker 18 μm carbon fibers. Carbon fiber fracture of the 8 μm diameter fiber shows complete disconnection, whereas the 18 μm fiber shows the maintenance of partial electrical contacts. It was considered that the complete disconnection of the electrical contact point was expected to occur in the case of thin 8 μm fiber fracture. On the other hand, the break of the thick 18 μm carbon fiber might have maintained an electrical contact until a higher strain level than for the 8 μm case.

Electrical Resistivity and AE of Multi-Carbon Fiber Composites. Figure 8(a) shows the electrical resistivity, electrical resistance difference ($\Delta R/R_0$) and stress as a function of the elapsed testing time and the applied strain in 8 μm ten-carbon fiber/epoxy composites. When the first fiber fracture occurred in each individual carbon fiber, the electrical resistivity increased stepwise in the ten-carbon fiber composites. Arrow marks indicate the first fracture of each individual fiber. The electrical resistivity plot exhibited the exact magnitude of the change due to the subsequent fiber fractures. The electrical resistance difference increased exponentially with the increase in the number of carbon fibers that had experienced the first fracture of each carbon fiber. This behavior might occur if the electrical resistance of the remaining fibers provided the dominant effect on the total electrical resistance.

In order to observe the increase in the electrical resistance, Figure 8(b) shows the change in logarithmic electrical resistance over equal time durations for each first fiber fracture in the ten-carbon fiber composite. As the number of fibers that had experienced the first fiber fracture increased at each individual fiber, the slope of the logarithmic electrical resistance increased. When the first individual fiber was broken in ten-carbon fiber composite, for example, one tenth of the total electrical resistance could increase. Next, one ninth of the measured electrical resistance for the remaining nine fibers could increase by fracture of the second fiber, and so on. Finally, one fiber fracture from two remaining fibers could increase the total electrical resistance almost twice compared to the three remaining fibers case.

Figure 9 shows the electrical resistance and AE signals depending on the ED treatment in the ten-carbon fiber composite. The electrical resistance change was in accordance with the detected AE

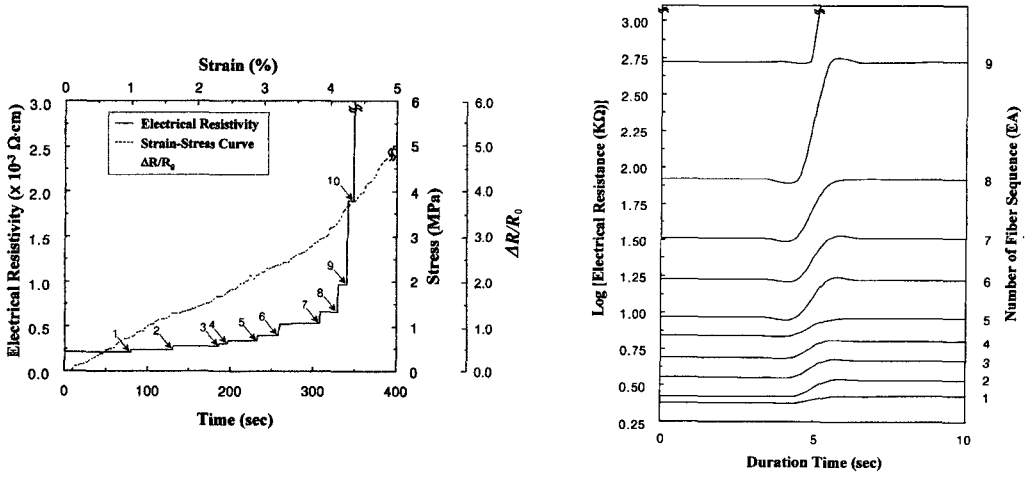

(a) (b)

Figure 8. Behavior of (a) electrical resistivity and electrical resistance difference ($\Delta R/R_0$); (b) logarithmic electrical resistance due to the first fracture of the individual fiber in the ten-carbon fiber composite.

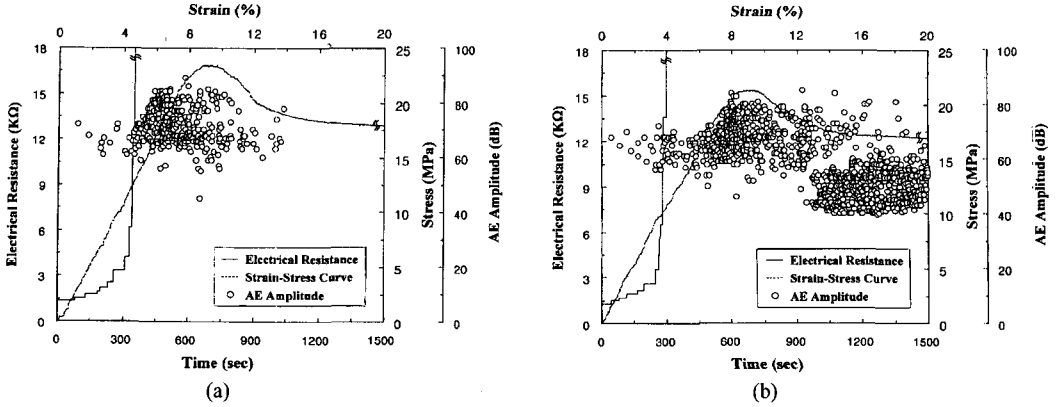

Figure 9. Comparison of electrical resistance and AE amplitude depending on the surface treatment in ten-carbon fiber composites: (a) the untreated; (b) the ED.

signals of the first fracture of the individual carbon fiber in both the untreated and the ED treated composites. The AE event number of high AE amplitude group in Figure 9(b) was larger than the number in Figure 9(a). Especially, the number of AE events from interlayer failure in the ED fiber composites exhibited a well-separated group, whereas the untreated composite did not show such an interlayer group.

Figure 10 shows photographs of typical microfailure modes of the ten-carbon fiber composite, depending on the ED treatment, at 8% strain. Figure 10 is (a) the untreated- and (b) the ED carbon fiber composites, and the many arrow marks indicate the position of the fiber fractures. The number of fiber fragments of the ED composite

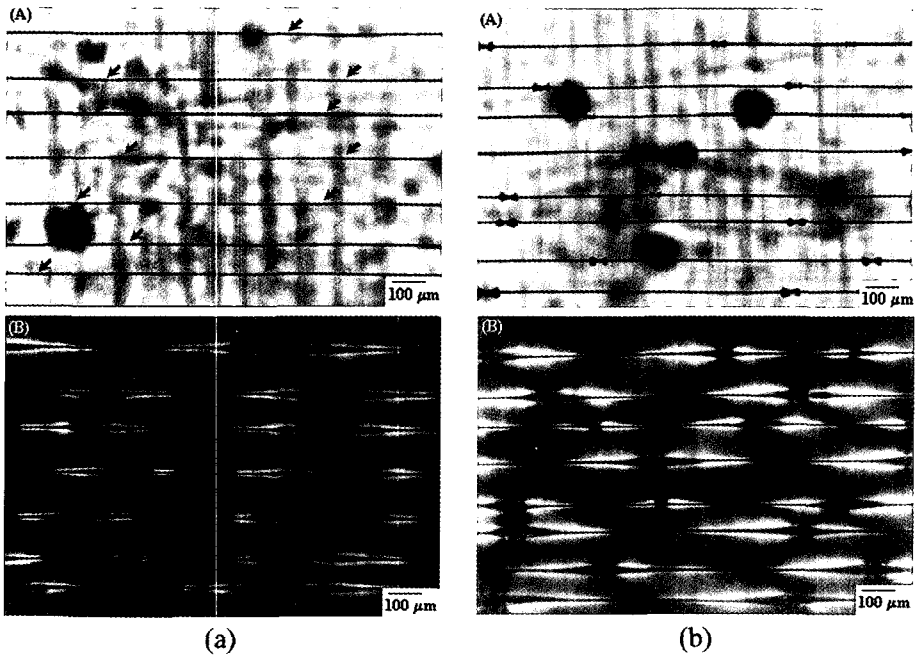

Figure 10. Comparison of microfailure modes depending on the surface treatment in ten-carbon fiber composites: (a) the untreated; (b) the ED.

was significantly larger than for the untreated case. This is based on better stress transfer phenomena from the matrix to the fiber in a birefringence pattern of the ED composite. Due to the different stress state, the fracture mode of the untreated- and the ED carbon fiber composite appeared as a debonding strip and a cone-shaped pattern, respectively. At the position of the fiber fracture, the untreated case showed a less developed stress whitening pattern with low angle, whereas the ED composite showed a fully developed stress whitening pattern with high angle.

Conclusions

Using two-fiber composites, the ED carbon fiber composite treated with PBMA exhibited a higher IFSS than the untreated composite. This might be expected due to the electrically and firmly adsorbed polymeric coating, as well as hydrogen and chemical bonding coming from polar functional groups such as carboxyl groups at two each interfaces. Many AE signals resulted from the interlayer failure and more fiber breaks occurred in the ED composite than in the untreated single- and ten-carbon fibers composite. The logarithmic electrical resistivity of the untreated case increased suddenly to infinity, whereas the ED composite increased more gradually to infinity. This might be because of the retarded fracture time due to improved interfacial adhesion. The logarithmic electrical resistivity curve of the thick fiber composite exhibited a rather broadly increasing trend compared to the thin fiber composite. The thick fiber composite may have maintained electrical contact until a higher strain level. As the number of fibers that had experienced first fiber fracture increased at individual fiber, the electrical resistance change increased exponentially in the ten-carbon fiber composites. The electrical resistivity depends on the microfailure mechanism and responds sensitively to geometry factors such as fiber diameter as well as the fiber treatment. Electro-micromechanical techniques combined with AE can be a useful method to evaluate interfacial properties of conductive carbon fiber reinforced composites nondestructively.

Acknowledgement. This work was supported financially by a Korea Research Foundation Grant (KRF-99-041-E00499).

References

(1) C. M. Baillie and M. G. Bader, *J. Mater. Sci.*, **29**, 3822 (1994).
(2) Z. F. Li, A. N. Netravali, and W. Sachse, *J. Mater. Sci.*, **27**, 4625 (1992).
(3) J. M. Park, J. O. Lee, and T. W. Park, *Polym. Compo.*, **17**, 375 (1996).
(4) J. O. Iroh, J. P. Bell, D. A. Scola, and J. P. Wesson, *Polymer*, **35**, 1306 (1994).
(5) J. A. King, D. A. Buttry, and D. F. Adans, *Polym. Compos.*, **14**, 301 (1993).
(6) H. T. Chiu and J. S. Lin, *J. Mater. Sci.*, **27**, 319 (1992).
(7) J. M. Park, Y. M. Kim, and K. W. Kim, *J. Colloid & Interf. Sci.*, **231**, 114 (2000).
(8) A. R. Sanadi and M. R. Piggott, *J. Mater. Sci.*, **20**, 431 (1985).
(9) S. I. Lee, J. M. Park, D. W. Shin, and D. J. Yoon, *Polym. Compos.*, **20**, 19 (1999).
(10) L. T. Drzal, *Mater. Sci. & Eng.*, **21**, 289 (1990).
(11) J. M. Park, W. G. Shin, and D. J. Yoon, *Compos. Sci. & Technol.*, **59**, 355 (1999).
(12) K. Yuse and C. Bathias, in *Proceedings of ICCM-12*, Paris, France, 1999, pp 767.
(13) X. Fu and D. D. L. Chung, *Compos. Interf.*, **4**, 197 (1998).
(14) X. Fu and D. D. L. Chung, *Cem. and Concr. Res.*, **25**, 1397 (1995).
(15) X. Wang and D. D. L. Chung, *Compos. Interf.*, **5**, 277 (1998).
(16) X. Wang and D. D. L. Chung, *Compos. Interf.*, **5**, 191 (1998).
(17) T. Prasse, F. Michel, G. Mook, K. Schulte, and Bauhofer, in *Proceedings of ICCM-12*, Paris, France, 1999, pp 556.
(18) J. M. Park, E. M. Chong, D. J. Yoon, and J. H. Lee, *Polym. Compos.*, **19**, 747 (1998).
(19) B. T. Ma, L. S. Schadler, C. Laird, and J. C. Figueroa, *Polym. Compos.*, **11**, 211 (1990).
(20) J. M. Park, J. W. Kim, and K. Goda, *Compos. Sci. & Technol.*, **60**, 439 (2000).
(21) L. T. Drzal, M. J. Rich, M. F. Koeing, and P. F. Lloyd, *J. of Adhesion*, **16**, 133 (1983).
(22) A. Kelly and W. R. Tyson, *Mech. and Phys. of Solids*, **13**, 329 (1965).
(23) K. Goda, J. M. Park, and A. N. Netravali, *J. Mater. Sci.*, **30**, 2722 (1995).